Colloids and Surfaces B: Biointerfaces 141 (2016) 491–498

Contents lists available at ScienceDirect

Colloids and Surfaces B: Biointerfaces

journal homepage: www.elsevier.com/locate/colsurfb

Osteogenic effect of controlled released rhBMP-2 in 3D printed porous hydroxyapatite scaffold

Hai Wang[a,1], Gui Wu[b,1], Jing Zhang[c], Kui Zhou[d], Bo Yin[a], Xinlin Su[a], Guixing Qiu[a], Guang Yang[e], Xianglin Zhang[d], Gang Zhou[c,**], Zhihong Wu[f,g,*]

[a] Department of Orthopaedic Surgery, Peking Union Medical College Hospital (PUMCH), Beijing 100730, China
[b] Department of Orthopaedics, First Affiliated Hospital, Fujian Medical University, Fujian 350108, China
[c] Key Laboratory for Biomechanics and Mechanobiology of Ministry of Education, School of Biological Science and Medical Engineering, Beihang University, Beijing 100191, China
[d] College of Materials Science and Engineering, Huazhong University of Science and Technology, Wuhan 430074, China
[e] College of Life Science and Technology, Huazhong University of Science and Technology, Wuhan 430074, China
[f] Central Laboratory, Peking Union Medical College Hospital (PUMCH), Beijing 100730, China
[g] Beijing Key Laboratory for Genetic Research of Bone and Joint Disease, Beijing 100730, China

ARTICLE INFO

Article history:
Received 11 January 2016
Received in revised form 2 February 2016
Accepted 3 February 2016
Available online 6 February 2016

Keywords:
3D printing
Hydroxyapatite (HA)
rhBMP-2
Controlled release
Osteogenic effect

ABSTRACT

Recently, 3D printing as effective technology has been highlighted in the biomedical field. Previously, a porous hydroxyapatite (HA) scaffold with the biocompatibility and osteoconductivity has been developed by this method. However, its osteoinductivity is limited. The main purpose of this study was to improve it by the introduction of recombinant human bone morphogenetic protein-2 (rhBMP-2). This scaffold was developed by coating rhBMP-2-delivery microspheres with collagen. These synthesized scaffolds were characterized by Scanning Electron Microscopy (SEM), a delivery test in vitro, cell culture, and the experiments in vivo by a Micro-computed tomography (μCT) scan and histological evaluation of VanGieson staining. SEM results indicated the surface of scaffolds were more fit for the adhesion of hMSCs to coat collagen/rhBMP-2 microspheres. Biphasic release of rhBMP-2 could continue for more than 21 days, and keep its osteoinductivity to induce osteogenic differentiation of hMSCs in vitro. In addition, the experiments in vivo showed that the scaffold had a good bone regeneration capacity. These findings demonstrate that the HA/Collagen/Chitosan Microspheres system can simultaneously achieve localized long-term controlled release of rhBMP-2 and bone regeneration, which provides a promising route for improving the treatment of bone defects.

1. Introduction

Repairing critical bone defects due to trauma, tumors, infection and so on, is still a major challenge for orthopedists. The application of autografts and allografts are restricted in clinics because of the limited supply, complications of donor site, and the risk of disease transmission [1,2]. Thus, tissue engineered bone (TEB) has drawn more and more attention as an alternative [3].

With the advantage of the controlled inner/outer architecture, pores, porosity, and interconnectivity, 3D printed scaffolds are becoming of increasing interest compared to traditional ones [3]. Vessels and nerves can easily grow into the scaffold for the integration of channels [4]. They have a remarkable potential for bone formation and healing [5,6]. Some of them, including a polycaprolactone (PCL) scaffold (Osteopore International Pte) and a polymethyl-methacrylate scaffold (OXPEKK-IG OsteoFab; Oxford Performance Materials), have been approved for commercial production by the Food and Drug Administration (FDA) [7,8]. Rapid prototyping (RP) technology (one of 3D printing technologies) is a good choice for fabricating TEB scaffolds due to its reliability and its reproducibility [9]. Polymer/ceramic composite scaffolds fabricated by RP techniques show enhanced mechanical properties and biocompatibility [10–12]. The stoichiometry of hydroxyapatite(HA) is similar to the inorganic part of natural bone, so it is a promising TEB [13]. In our previous studies, a new porous HA ceramic scaffold has been fabricated by the micro-syringe extrusion

* Corresponding author at: Central Laboratory, Peking Union Medical College Hospital, No. 1 Shuaifuyuan Hutong, Beijing 100730, China.
** Corresponding author at: Key Laboratory for Biomechanics and Mechanobiology of Ministry of Education, School of Biological Science and Medical Engineering, Beihang University, Xueyuan 37, Beijing 100191, China.
E-mail addresses: zhougang@buaa.edu.cn (G. Zhou), wuzh3000@126.com (Z. Wu).
[1] The first two authors contributed equally to this article.

http://dx.doi.org/10.1016/j.colsurfb.2016.02.007

system, a RP technique [14]. Its biocompatibility and osteoconductivity have been confirmed before, but the osteoinductivity is still limited [14,15]. Thus, it's very important to functionalize this scaffold to accelerate the bone healing process.

Bone morphogenetic proteins(BMPs), members of the transforming growth factor beta (TGF-ß) superfamily, have osteoinductive property, and two of them (BMP-2 & BMP-7) are widely available commercially [16]. Specifically, BMP-2 shows a very strong osteoinductive activity [17]. Thus, the introduction of recombinant human bone morphogenetic protein-2 (rhBMP-2) to this HA scaffold could potentially enhance its osteoinductivity. But, rhBMP-2 alone cannot induce bone regeneration because of its short retention [18]. A collagen sponge is suggested for rhBMP-2 by the manufacturer. Adverse effects may rise at an excessively high dose, which is aimed to overcome its rapid diffusion [19]. Long-term delivery of rhBMP-2 could enhance the osteogenic efficacy as compared with the short-term delivery [20]. A suitable delivery system of rhBMP-2 plays a key role to ensure its controlled release and the bioactivity. Previously, we have prepared chitosan microspheres (CMs) containing encapsulated BMP-2 or synthetic peptide derived from BMP-2 [21,22]. Through the introduction of CMs loaded with BMP-2 and BMP-2-derived synthetic peptide, the composite could induce obvious ectopic bone formation.

In this study, we hypothesized that the introduction of rhBMP-2 through CMs can provide the 3D printed porous HA scaffold with the osteoinductivity. To test it, a porous HA scaffold fabricated by RP technique was coated with rhBMP-2CMs by collagen. We demonstrate that controlled release of rhBMP-2 could induce Human Mesenchymal Stem Cells (hMSCs) for osteogenic differentiation in vitro and ectopic bone formation in vivo.

2. Materials and methods

2.1. Materials

HA powder (MH-HAP) was obtained from Nanjing Emperor Nano Material Co., Ltd., China. rhBMP-2 was obtained from Medtronic, Inc., USA. Type I collagen (C9879), 1-ethyl-3-[3-dimethylaminopropyl] carbodiimide hydrochloride (EDC), *N*-hydroxysuccinimide (NHS), and chitosan were purchased from Sigma-Aldrich Co., USA.

2.2. Fabrication of porous HA scaffolds

The elliptic cylindrical porous HA scaffold of $15 \times 7 \times 5\,mm^3$ with 500 μm pores was prepared as previously described [14]. Briefly, the specifications of the scaffold were predefined using the extrusion deposition system (MAM-II, Fochif, China). 30vol% HA slurry extruded from the conical nozzle and constructed in a layer by layer process under the control of computer. The scaffolds were air dried for 24 h at room temperature after the construction was completed. Then, the scaffolds were sintered in a 1.4 kW, 2.45 GHz microwave furnace (Hamilab-V1500, Syno-therm. Co. Ltd., China) using the following procedure: temperature increased to 400 °C slowly (2 °C/min) for 1 h at first, then increased to 1200 °C rapidly for 30 min to improve the strength of the scaffold, and at last, cooled to room temperature.

2.3. Preparation of CMs containing rhBMP-2

CMs containing rhBMP-2 were prepared with the emulsion cross-linking method as previously described [21,22]. Briefly, 3% (w/v) span, 2.4% (w/v) tween and 3% (w/v) magnesium stearate were dissolved in liquid paraffin to obtain the oil phase. And the above mixture was stirred at 45 °C using water bath for 1 h. 450 mg chitosan and 4 mg rhBMP-2 was dispersed in 2% (V/V) aqueous acetic acid solution and agitated for 30 min. Thereafter, the chitosan solution was dropped into the liquid paraffin slowly. One gram of 3-methoxy-4-hydroxybenzaldehyde (vanilline) was dissolved in 2 ml alcohol and added to the W/O emulsion. The emulsion was stirred for 6 h. The obtained microspheres were washed with petroleum ether and isopropanol to remove the remaining solvent, and then lyophilized for 18 h.

2.4. Synthesis of scaffolds coated with collagen/CMs

Collagen I was dissolved in acetic acid (0.05 M) to obtain a concentration of 0.1 g/ml. The sterilized HA scaffolds were soaked in the collagen solution and put in a vacuum drying oven for vacuum aspiration for 24 h. First, both EDC and NHS were added in MES-buffered solution (pH 5.5) with a EDC:NHS ratio of 4:1 (w/w). Then, the solution with 2.5 mg/ml EDC and 0.63 mg/ml NHS was added to the collagen solution to cross-link the collagen. After incubating for 4 h, the HA/Collagen scaffolds were dried at 37 °C for 6 h. Thereafter, the HA/Collagen (HC) scaffolds were washed with phosphate buffer solution (PBS, pH 7.4, Gibco inc., USA). The coating process was performed under sterilized condition.

The synthesis of HA scaffold coated with collagen/rhBMP-2CMs (HCC) was prepared using a previously described post-seeding technique [23]. CMs were suspended with deionized water at a concentration of 50 mg/ml. 50 μl of the suspension was dripped on the collagen coated scaffold carefully, and then the scaffold was dried and stored at −20 °C until use.

2.5. SEM observation of scaffolds

The lengths of HA scaffolds before and after sintering were measured to calculate the linear shrinkage. The pore size was measured using an inverted fluorescence microscope. Five pores were randomly selected in a ×10 view for each sample. The average length of the pores was calculated as the actual pore size. The microstructures of HA, HC and HCC scaffolds were observed by a Scanning electron microscopy (SEM, S-2400; Hitachi, Japan).

2.6. In vitro drug release

In vitro release of rhBMP-2 from the HCC composite scaffolds were carried out at 37 °C in 2 ml of PBS. At pre-determined intervals, the release medium was withdrawn and renewed with a fresh medium each time. The in vitro release kinetics of rhBMP-2 from HCC scaffolds was examined for 21 days. 2 ml PBS containing rhBMP-2 at 0.5, 1, 2, 4, 7, 14 and 21 days was all collected and replaced with equal amount of fresh PBS. Samples were stored at −20° C until the test. To determine the total amount of rhBMP-2 at each scaffold, the microspheres on the scaffold were dissolved with 500 μl of acetic acid (0.2 M), and then the solution was diluted with 3.5 ml PBS. All collected samples were centrifuged and filtered to remove the free floating microspheres and quantitatively analyzed using a Human BMP2 ELISA Kit (Sigma-Aldrich Co., USA) at the end of the experiment. The experiments were run in triplicate per time point. Three scaffolds were measured here in total.

2.7. Cell viability

hMSCs (Third passage, ScienCell Research Laboratories, USA) were incubated in Mesenchymal Stem Cell Medium (MSCM, ScienCell Research Laboratories, USA) with Penicillin and Streptomycin solution (Gibco inc., USA) as described by Li et. al. [24]. For cell seeding, HA, HC and HCC scaffolds were sterilized under UV light for 2 h and washed with PBS three times. hMSCs were seeded in a 96-well plate at a density of 5000 cells/well. 200 μl of MSCM was added to each well. The sterilized HA, HC and HCC scaffold was put into the

well, and the culture medium was changed every 3 days. The cells cultured with MSCM without a scaffold were set as a control. On days 1, 3 and 7 of culture, three scaffolds were removed separately, and the cells were rinsed with PBS. CCK-8 reagent (Dongjindo Molecular Technologies, inc., Japan) was diluted with MSCM at a ratio of 1:10(v/v) and 100 μl of the MSCM containing CCK-8 reagent was added to each well. After 2 h of incubation at 37 °C, the optical density of cell proliferation was measured with a microplate reader at 450 nm.

2.8. Immunofluorescent assay

Concentration of hMSCs were adjust to 1×10^6 cells/ml. Fifty microliters of the MSCs were dipped on the HA, HC and HCC scaffold respectively, and incubation in a 24-well plate for 30 min. Then 950 μl of MSCM was added to each well. After incubated for 24 or 48 h, the media was gently removed and the specimens were washed with PBS. The cells on the scaffolds were fixed with 4% paraformaldehyde (Gibco inc., USA) for 10 min. PBS was used to wash the specimen at each subsequent steps. Triton(0.2%, w/v) was used to increase the permeabilization of the cells for 5 min, and then nonspecific binding was blocked by 1% BSA for 30 min. Anti-β-Tubulin Mouse Monoclonal Antibody (Abcam plc, UK) was added to combine with the cytoskeleton protein for 60 min. After washing with PBS for 3 times, the specimens were incubated with goat anti-mouse IgG(Zhong Shan Golden Bridge Biotechnology, China). The 4′,6-diamidino-2-phenylindole (DAPI) solution (Sigma-Aldrich Co., USA) was added to each well for 5 min before the scaffolds were observed with the fluorescence microscope.

2.9. Alkaline phosphatase (ALP) activity

The ALP activity of hMSCs was used to determine the bioactivity of the released rhBMP-2. The HCC scaffolds were soaked in 5 ml MSCM for 1, 3 or 7 days, respectively. At each time point, the scaffold was removed, the culture medium was centrifuged and the supernatant was collected after sterilization with a 0.22 μm filter. hMSCs were seeded in a 96-well plate (10000 cells/well), and then incubated overnight. The culture medium was refreshed with the collected MSCM above or MSCM without rhBMP-2(control group). The cells were washed with PBS and lysed in 0.2% Triton X–100 in distilled water for 20 min at room temperature after culturing for 7 days. The ALP activity of each well was calculated using QuantiChrom TM Alkaline Phosphatase Assay Kit (BioAssay Systems, USA). The absorbance was measured using microplate reader (Synergy H1) at 405 nm. The ALP activity was normalized by the total intracellular protein production which was tested strictly according to the instructions of Pierce BCA Protein Assay Kit (Thermo scientific, USA).

2.10. In vivo experiment

Animal experiments were approved by the animal ethics committee of Peking Union Medical College Hospital (PUMCH), China. All procedures were performed in accordance to specifications of guidelines for the care and maintenance of animals. Twenty-four New Zealand rabbits (2.5 to 3.0 kg, Experimental Animal Center of PUMCH, China), age 3 ~ 6 months, were anesthetized with an intravenous injection of 3% pentobarbital sodium (1 ml/kg body weight, Sigma, USA). A 2 cm skin incision from the groin midpoint to the knee was taken, and the myolemma was longitudinally split. After implanting scaffolds into the intramuscular gap, muscle and skin were sutured with 3–0 silk sutures. 800,000IU penicillin sodium (North China Pharmaceutical Group Corporation, China) was injected intramuscularly before and after operation for 3 days to prevent infection. 0.15 mg buprenorphine (Tianjin Institute of Pharmaceutical Research, China) was also applied to relieve pain every 12 h for 3 days. Animals were sacrificed after 4 and 8 weeks respectively ($n = 4 \times 3 \times 2$). Samples were removed and fixed in 4% paraformaldehyde.

2.11. Evaluation of bone regeneration capability

Three-dimensional images of bone regenerated in the scaffolds were visualized with the Micro-computed tomography (μCT) scans (SkyScan 1076, Belgium). Samples were scanned at a slice interval of 9 μm, energy of 70 kV, and current of 139 μA. The 2-dimensional images were acquired with the NRecon software (Version 1.5, Bruker Corporation, USA) and analyzed with the CT Analyser software (Version 1.8, Bruker Corporation, USA). Trabecular thickness (Tb.Th), Bone volume (BV), and Bone volume/Tissue volume (BV/TV) were calculated in the regions of interest (ROI) generated based on the scaffold margin. The thresholds of bone and HA scaffold were set at 148–661 and 661–3040 respectively. At last, they were reconstructed and submitted to the Mimics 10.0 software (Materialise, Belgium) for processing to produce the 3-dimensional images of bone regenerated.

2.12. Histological evaluations

The histological specimens were fixed in 4% paraformaldehyde for 7 days, dehydrated with ethyl alcohol, embedded in methylmethacrylate (MMA), and sectioned transversely at a thickness of 50 μm with the Leica SP1600 saw microtome (Leica Biosystems, German). The slides were stained with VanGieson for histological evaluations. The bone formations in the scaffolds were observed using a microscope and a digital camera (Leica Microsystems).

2.13. Ethics statement

All experiments involving the use of animals were in compliance with Provisions and General Recommendation of Chinese Experimental Animals Administration Legislation and were approved by Beijing Municipal Science & Technology Commission (Permit Number: SCXK (Beijing) 2006-0008 and SYXK (Beijing) 2006-0025).

2.14. Statistical analysis

Data was expressed as mean ± standard deviation (SD). Samples of each group were performed in triplicate. One-way ANOVA was used to analyze the differences among groups. A $P < 0.05$ value was considered as statistically different.

3. Results

3.1. Characteristics of scaffolds

As designed, porous HA scaffolds were successfully fabricated by the combination of extrusion deposition technique and microwave sintering. After sintering, the scaffold dimensions were reduced from $15 \times 7.4 \times 5.5\,mm^3$ to $10.5 \times 5.2 \times 3.85\,mm^3$ (Fig. 1). The shrinkage of the structure after sintering was about 34.4% in all directions. The cross-section SEM image of HA scaffold illustrated that the pores were interconnected with a diameter of approximately 460 μm. In HC scaffolds, a thin layer of collagen was uniformly adhered to HA surface to modify it. In HCC scaffolds, scaffolds were successfully coated with 10 μm spherical CMs containing rhBMP-2 by collagen.

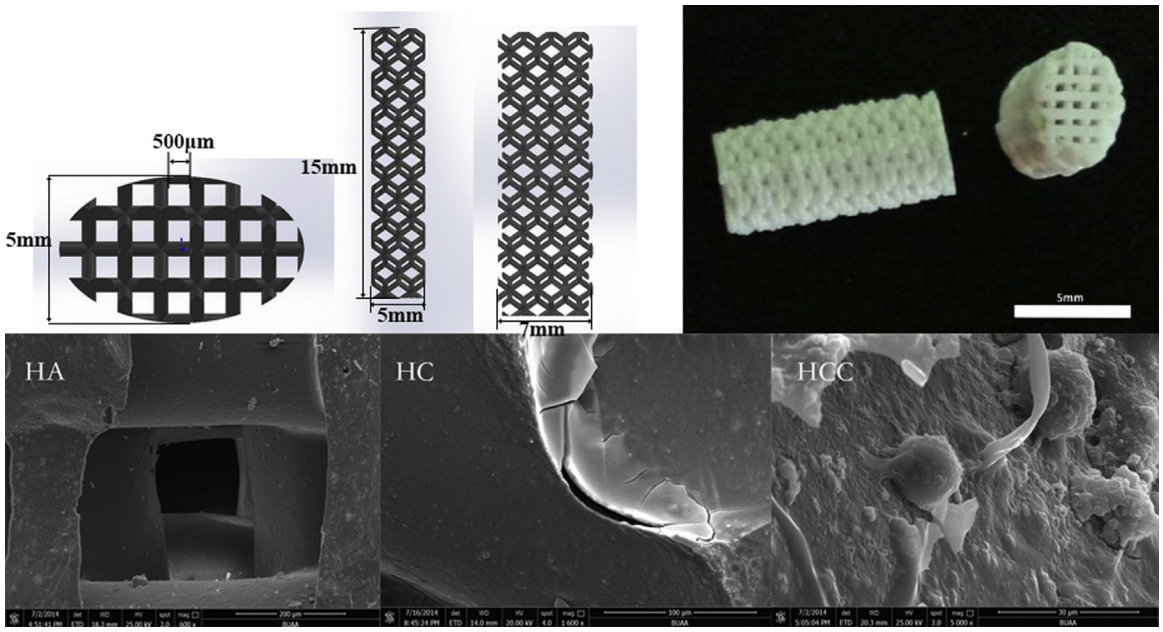

Fig. 1. Design drawing ($15 \times 7 \times 5\ mm^3$) and SEM images of scaffolds.

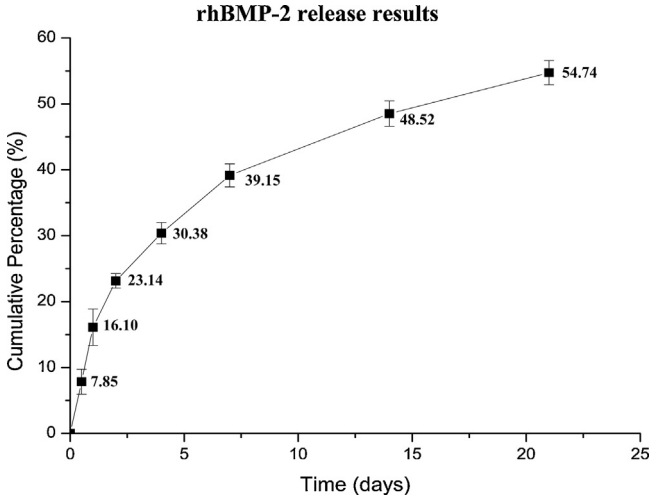

Fig. 2. rhBMP-2 release profile of the HCC scaffold coating with rhBMP-2 microspheres.

3.2. Release profile of rhBMP-2 in vitro

In vitro release of rhBMP-2 from the HCC scaffold was carried out in PBS buffer solution at 37 °C. To efficiently keep the therapeutic effect of rhBMP-2, it is crucial to ensure that pristine rhBMP-2 can be released from the scaffold. Hydrazone bonds can be reversibly cleaved to aldehyde and hydrazine groups under a weakly acidic environment. Since rhBMP-2 contains a hydrazine group, a hydrazone bond is a suitable linker to covalently conjugate rhBMP-2 to HA-collagen. When the hydrazone bone was broken, rhBMP-2 can be gradually released from the HCC scaffold. The average amount of rhBMP-2 in the scaffolds was 3.63 ± 0.24 μg measured by dissolving with acetic acid. Fig. 2 shows the kinetic release of rhBMP-2 in vitro. The release of rhBMP-2 had a unique biphasic profile of an initial burst release (phase I) in the first seven days and a secondary sustained release (phase II) after that. Total of 1.98 ± 0.17 μg (54%) was continuously released from the HCC scaffold during 21 days. Approximately 50% of rhBMP-2 was cumulatively released in phase I, and then the release rate was gradually decreased with time. During 21days, the concentration of released rhBMP-2 was above 112.8 ng/ml at each tested time point. These results verify that chemical conjugation of rhBMP-2 to polymeric CS microsphere can efficiently avoid initial burst release and enhance long-term drug release in a controlled manner. The long-term controlled drug release should benefit from long degradation time of CS and the resulted weakly acidic compartment after CS microspheres degradation. So the drug delivery system based on the scaffold meets the demand of long-term drug treatment for bone defects.

3.3. Cell viability

The hMSCs proliferation results on days 1, 3 and 7 determined by CCK-8 assay are shown in Fig. 3. The results show that all three scaffolds are conducive to cell duplication with no significant difference ($p > 0.05$) on days 1, 3 and 7 of culture. There were more cells in the scaffolds with time. The morphology and proliferation of hMSCs that adhere to the surface of the scaffolds are shown in Fig. 4. The numbers of cells stained with DAPI on the surfaces of HC and HCC scaffolds were more than that of HA scaffolds after 24 and 48 h of culture, especially for HCC scaffolds. hMSCs extended their pseudopodia to closely cling to the surface in the HCC scaffold by β-tubulin staining. Based on these results, it could be seen that collagen and CMs were favorable for cell adhesion and expansion.

3.4. ALP activity

ALP activity was measured as a marker of osteogenic differentiation for hMSCs. As shown in Fig. 3, the leaching solution of the HCC scaffold could enhance the ALP activity as compared to control, and it increased with increasing culture time.

3.5. Ectopic bone formation

Besides evaluating drug release, the capability of bone regeneration was also investigated simultaneously when the scaffolds were implanted intramuscularly. Bone defect regeneration capability of the composite scaffolds was evaluated by X-ray microradiography and histological analysis. The results of μCT showed the newly ectopic bone formation in scaffolds was significantly enhanced

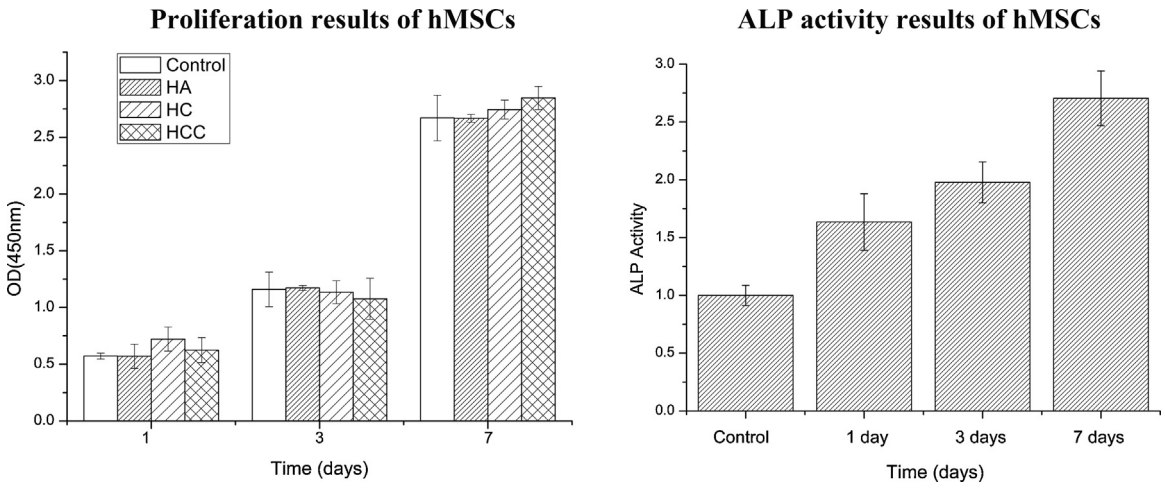

Fig. 3. Results of hMSCs culture: proliferation results of hMSCs co-culture in scaffolds & ALP activity results of hMSCs co-culture with the leaching solution of the HCC scaffolds (set control = 1).

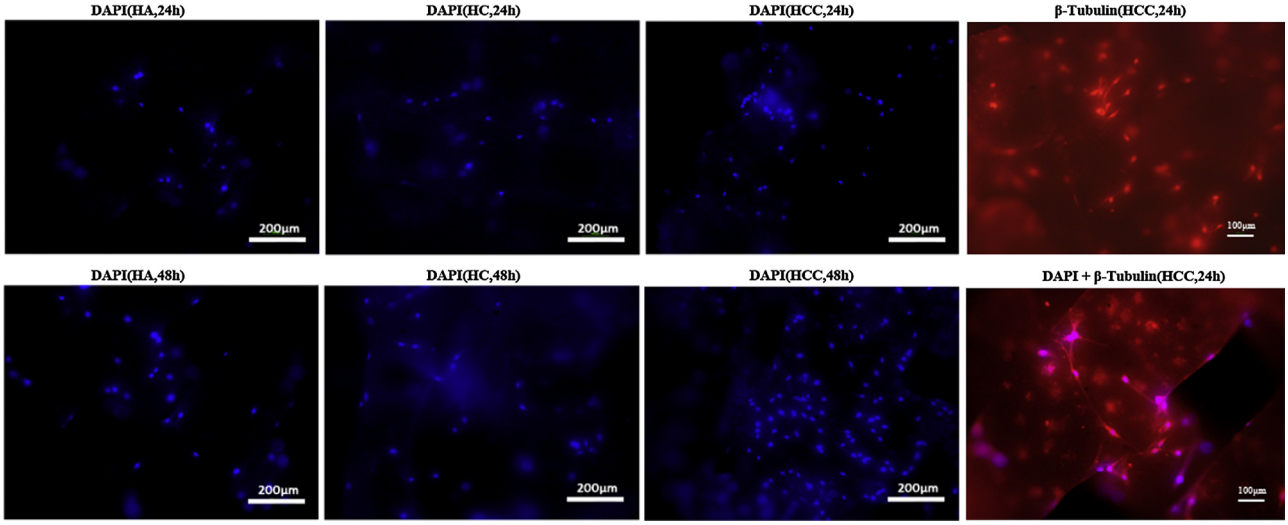

Fig. 4. Fluorescence microscope images of hMSCs stained with DAPI and/or β-Tubulin on the surfaces of the HA, HC and HCC scaffolds.

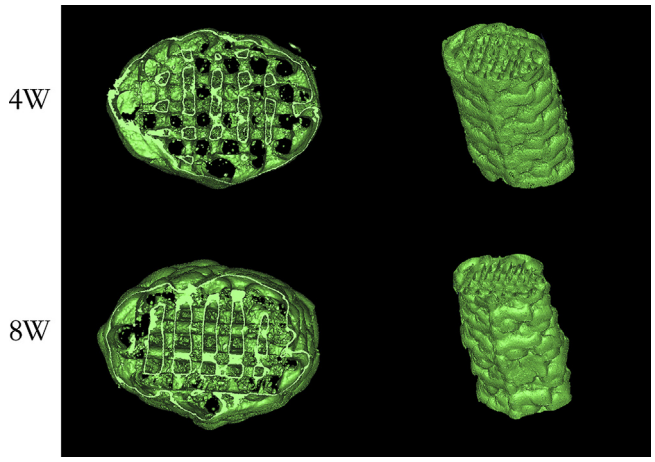

Fig. 5. μCT results of HCC scaffolds after implanting for 4 and 8 weeks.

after coating of rhBMP-2CMs in HCC scaffolds compared to HA and HC scaffolds (Fig. 5). Further quantitative analysis with μCT showed Tb.Th, BV, and BV/TV of HCC scaffolds were all increasing with time (Table 1). They were confirmed by the histological results (Fig. 6).

Table 1
The quantitative analysis results of μCT for HCC scaffolds.

	4 weeks	8 weeks	*P*
BV (mm^3)	4.69 ± 1.09	7.12 ± 1.56	0.04
BV/TV (%)	11.56 ± 1.22	17.14 ± 2.26	0.01
Tb.Th(mm)	0.074 ± 0.05	0.083 ± 0.05	0.04

It showed that ectopic bone formation was induced by sustained delivery of rhBMP-2 compared to no delivery. No bone formation with only fibrous tissues was observed in HA and HC scaffolds after 4 and 8 weeks. In contrast, the implantation of rhBMP-2CMs coated HA (HCC) scaffolds resulted in extensive bone formation, with a lot of osseous/osteoid tissue. Osseous tissue was located around the pores with osteoid tissue in the center. The results from X-ray microradiography and histological analysis robustly illustrated that the rhBMP-2-loaded scaffold also possesses excellent bone regeneration capability.

4. Discussion

In bone tissue engineering, there are three elements including scaffold, factors and seeding cells, where the scaffold is the most

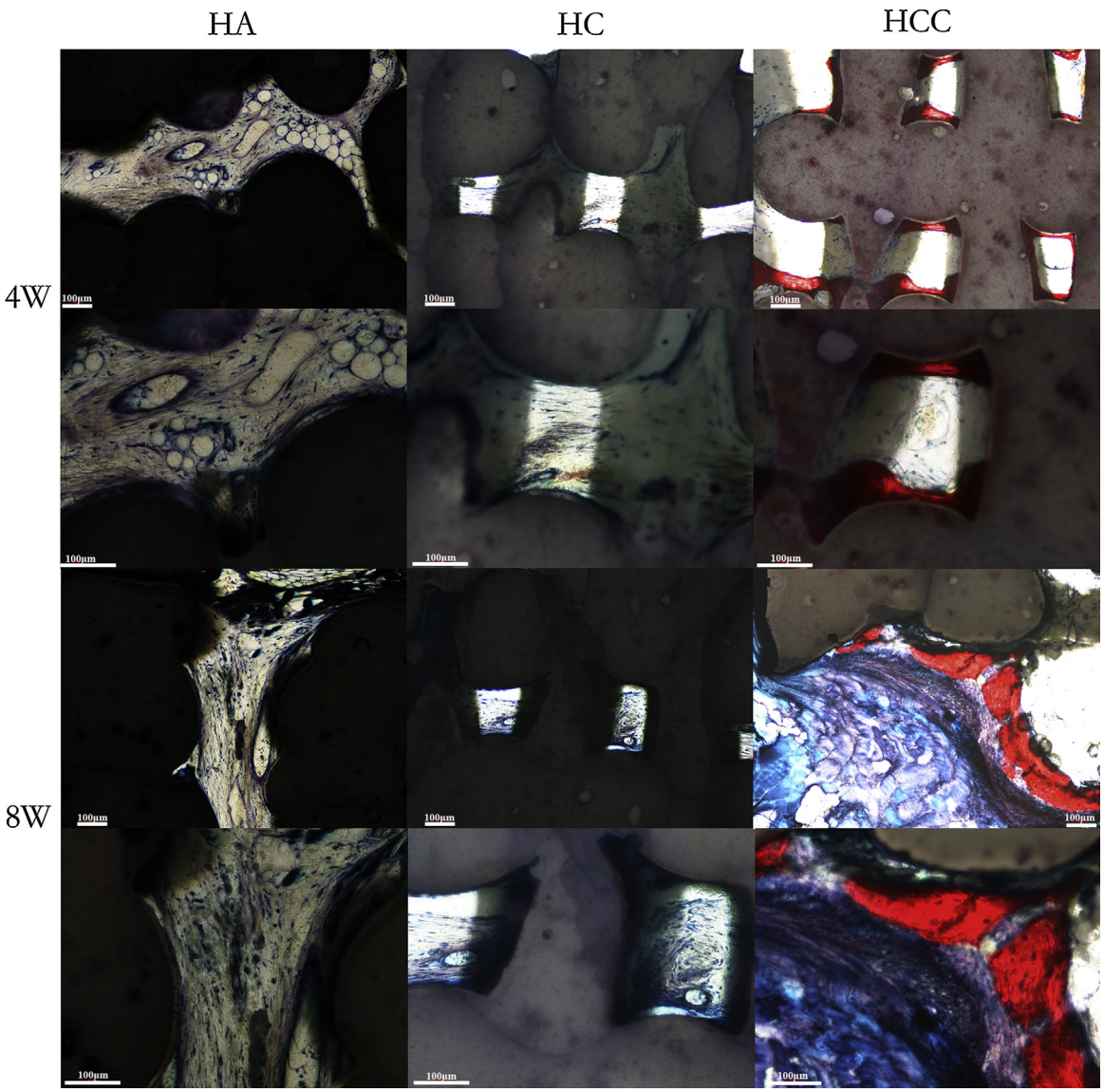

Fig. 6. Histological results of the HA, HC and HCC scaffolds stained with VanGieson after implanting for 4 and 8 weeks.

basic one. Traditional scaffolds cannot be adapted to the exact shape of the individual osseous defect [4]. Their microstructure including pore size, porosity, connectivity and pore shape affects the ingrowth of bone tissue and the mechanical property of the scaffold [25]. However, they are not able to be accurately controlled by traditional methods [26]. Using computer-assisted 3-D printing, an emerging RP technique, individual shaped 3-D ceramic scaffolds can be tailored with precise dimensions and highly defined and regular internal characteristics. Pure HA is one of the best materials for regeneration of new bone [27]. Previously, a more soluble HA ceramic scaffold has been fabricated by extrusion deposition technique and microwave sintering techniques [14]. As shown in Fig. 1, these porous HA scaffolds possessed good inner/outer architecture, and interconnective pores for bone ingrowth, although they had a certain degree of shrinkage after sintering.

The osteoinductivity of this porous HA scaffold should be enhanced, although the biocompatibility and osteoconductivity had been confirmed before [14]. BMPs are bone growth factors synthesized and secreted by osteoblasts, and can induce differentiation of mesenchymal cells into osteoblasts, stimulating osteogenesis in remodeling and healing processes [28]. It has been reported that rhBMP-2 and rhBMP-7 have the satisfactory osteoinductive property. Thus, introduction of rhBMP-2 to this scaffold would probably facilitate the scaffold with osteoinductivity, and enhanced the ingrowth of bone tissue.

A controlled and localized delivery system for a small amount of rhBMP-2 should be fabricated, because rhBMP-2 is rapidly degraded with a short half-life (7–16 min) in vivo [29]. To overcome this, an excess dosage of rhBMP-2 is an alternative, but it is expensive and can cause undesirable side-effects [30]. In this study, rhBMP-2CMs of 10–20 μm were successfully prepared via an emulsion cross-linking method as a potential drug/protein delivery system. After coating to HA surface by collagen, they showed a controlled delivery of rhBMP-2 in HCC scaffolds. Every HCC scaffold contained only 3.63 ± 0.24 μg rhBMP-2, much less than the dosage recommended by Medtronic. rhBMP-2 could release from the HCC scaffold continuously for over 21 days in vitro, and even then, the concentration of released rhBMP-2 (112.8 ng/ml) was still higher than the minimum concentration (10 ng/ml) which could upregulate osteogenesis of MSCs [31]. Therefore, CMs/Collagen/HA was a suitable delivery system for rhBMP-2.

The release kinetic of rhBMP-2 in this study showed a unique biphasic profile of an initial burst release (phase I) and a secondary sustained release (phase II). It was speculated that phase I was

mainly derived from the direct diffusion of rhBMP-2 in CMs and the release in phase II was most likely attributed to the diffusion through collagen. Initially, a sustained release was thought to be fit for inducing osseous formation [32]. Recent studies confirmed that a transient burst release followed by a sustained release could be even better than a continuously sustained release [33–36]. The burst release could possibly correlate with the retaining and inducing of host cells to the scaffolds and the sustained release might have the function to coordinate distribution of cells inside the scaffolds [36]. It was consistent with the biphasic profile of BMP-2 during the healing process of bone fracture in vivo [37]. The unique biphasic release profile of rhBMP-2/CMs/Collagen are favorable for bone formation in porous HA scaffolds.

No material, including rhBMP-2, collagen, and chitosan, could influence the cell viability of the MSCs [31,38]. That is why there was no significant difference in cell proliferation among these three groups and the number of cells increased with culture time. As expected, coating porous HA scaffolds with a collagen layer favored adhesion and growth of hMSCs. Collagen as a primary protein of bone tissue had excellent cell adhesion, biodegradability and biocompatibility [39]. It is an effective method to enhance the adhesion of cells to scaffolds by coating with collagen [40]. Hence, the number of cells attaching on the surface of HA scaffolds was less than the two others. More cells adhering on the HCC surface might be associated with more roughness of HCC scaffolds by CMs coating. The suitable attachment of hMSCs is a prerequisite of a successful tissue engineering [41].

The hypothesis of this study was that rhBMP-2 controlled release made porous HA scaffolds with osteoinductivity. To verify it, the differentiation ability of the released rhBMP-2 was measured in vitro using hMSCs. ALP, an ectoenzyme produced by osteoblasts, was selected as a maker to verify the osteogenic differentiation. The result suggested that the released rhBMP-2 still retained its bioactivity after encapsulating into CMs/collagen/HA scaffold, and the ALP activity was continuously elevated. It was closely related to the release profile of rhBMP-2 in vitro because the osteoinductivity of rhBMP-2 was in a dose-dependent manner [31]. In the first 7 days, the cumulative amount of released rhBMP-2 kept rising.

To further confirm the hypothesis, an experiment of ectopic bone formation in vivo was performed in this study. Scaffolds of three different types (HA, HC and HCC) were implanted intramuscularly respectively for 4 or 8 weeks. As shown in the results of μCT and histological slices, new bone tissue could be observed alone in the rhBMP-2-loaded scaffolds (HCC). The bone regeneration effect was observed in week 4, and continuously increased until 8weeks by quantitative analysis of μCT. Because only rhBMP-2 had the unique property of ectopic bone formation [42]. Histological results showed that osseous tissue was in the periphery of the pores, and osteoid tissue was in the center of the pores. It suggested that newly regenerated bone was induced by rhBMP-2 released from CMs on the surface of scaffolds.

5. Conclusions

The morphology, structure and mechanical property of the scaffold were rationally designed and tailored to be favorable for long-term drug controlled release and bone regeneration. In this study, a 3D printed porous HA scaffold with embedded rhBMP-2-delivery microspheres to improve cell differentiation capabilities was developed. The cytological assay indicated that the composite system possesses a good cell biocompatibility and osteoinductivity to induce osteogenic differentiation of hMSCs in vitro. The in vitro drug release experiment showed that rhBMP-2 could be released gradually from the composite for more than 21 days. In addition, in vivo experiment showed that the scaffold also works well to repaire bone defects. These results demonstrate the composite scaffold drug delivery system can simultaneously achieve localized long-term drug controlled release and bone regeneration, which is promising for the reconstruction of complex bony defects.

Acknowledgements

Thanks Michael Anderson (Department of neuroscience, School of Medicine, Johns Hopkins University) for language editing. This study was financially supported by National High Tech Research and Development Program (863 program, 2015AA020316, 2015AA033601), and Beijing Science Foundation (Z151100003715006).

Appendix A. Supplementary data

Supplementary data associated with this article can be found, in the online version, at http://dx.doi.org/10.1016/j.colsurfb.2016.02.007.

References

[1] A.J. Aho, T. Ekfors, P.B. Dean, H.T. Aro, A. Ahonen, V. Nikkanen, Incorporation and clinical results of large allografts of the extremities and pelvis, Clin. Orthop. Relat. Res. (1994) 200–213.
[2] J.P. Beier, R.E. Horch, A. Hess, A. Arkudas, J. Heinrich, J. Loew, H. Gulle, E. Polykandriotis, O. Bleiziffer, U. Kneser, Axial vascularization of a large volume calcium phosphate ceramic bone substitute in the sheep AV loop model, J. Tissue Eng. Regen. Med. 4 (2010) 216–223.
[3] J.W. Lee, K.S. Kang, S.H. Lee, J.Y. Kim, B.K. Lee, D.W. Cho, Bone regeneration using a microstereolithography-produced customized poly(propylene fumarate)/diethyl fumarate photopolymer 3D scaffold incorporating BMP-2 loaded PLGA microspheres, Biomaterials 32 (2011) 744–752.
[4] P.H. Warnke, H. Seitz, F. Warnke, S.T. Becker, S. Sivananthan, E. Sherry, Q. Liu, J. Wiltfang, T. Douglas, Ceramic scaffolds produced by computer-assisted 3D printing and sintering: characterization and biocompatibility investigations, J. Biomed. Mater. Res. B: Appl. Biomater. 93 (2010) 212–217.
[5] A. Yeo, E. Sju, B. Rai, S.H. Teoh, Customizing the degradation and load-bearing profile of 3D polycaprolactone-tricalcium phosphate scaffolds under enzymatic and hydrolytic conditions, J. Biomed. Mater. Res. B: Appl. Biomater. 87 (2008) 562–569.
[6] L. Shor, S. Guceri, R. Chang, J. Gordon, Q. Kang, L. Hartsock, Y. An, W. Sun, Precision extruding deposition (PED) fabrication of polycaprolactone (PCL) scaffolds for bone tissue engineering, Biofabrication 1 (2009) 015003, http://dx.doi.org/10.1088/1758-5082/1/1/015003.
[7] K.H. Schuckert, S. Jopp, S.H. Teoh, Mandibular defect reconstruction using three-dimensional polycaprolactone scaffold in combination with platelet-rich plasma and recombinant human bone morphogenetic protein-2: de novo synthesis of bone in a single case, Tissue Eng. Part A 15 (2009) 493–499.
[8] S.M. Kurtz, S. Kocagoz, C. Arnholt, R. Huet, M. Ueno, W.L. Walter, Advances in zirconia toughened alumina biomaterials for total joint replacement, J. Mech. Behav. Biomed. Mater. 31 (2014) 107–116.
[9] M.T. Arafat, C.X. Lam, A.K. Ekaputra, S.Y. Wong, X. Li, I. Gibson, Biomimetic composite coating on rapid prototyped scaffolds for bone tissue engineering, Acta Biomater. 7 (2011) 809–820.
[10] J.J. Blaker, J.E. Gough, V. Maquet, I. Notingher, A.R. Boccaccini, In vitro evaluation of novel bioactive composites based on bioglass-filled polylactide foams for bone tissue engineering scaffolds, J. Biomed. Mater. Res. A 67 (2003) 1401–1411.
[11] J.D. Kretlow, A.G. Mikos, Review: mineralization of synthetic polymer scaffolds for bone tissue engineering, Tissue Eng. 13 (2007) 927–938.
[12] L. Shor, S. Guceri, X. Wen, M. Gandhi, W. Sun, Fabrication of three-dimensional polycaprolactone/hydroxyapatite tissue scaffolds and osteoblast-scaffold interactions in vitro, Biomaterials 28 (2007) 5291–5297.
[13] B. Leukers, H. Gulkan, S.H. Irsen, S. Milz, C. Tille, M. Schieker, H. Seitz, Hydroxyapatite scaffolds for bone tissue engineering made by 3D printing, J. Mater. Sci. Mater. Med. 16 (2005) 1121–1124.
[14] Q. Wu, X.L. Zhang, B. Wu, W. Huang, Effects of microwave sintering on the properties of porous hydroxyapatite scaffolds, Ceram. Int. 39 (2013) 2389–2395.
[15] H. Wang, L. Zhang, G. Qiu, W. Huang, K. Zhou, X. Zhang, Z. Wu, [Effects of bore diameter of porous hydroxyapatite scaffolds on three-dimensional dynamic cultivation of osteoblasts], Zhonghua Yi Xue Za Zhi 94 (2014) 3098–3101.
[16] K.C. Nune, A. Kumar, L.E. Murr, R.D. Misra, Interplay between self-assembled structure of bone morphogenetic protein-2 (BMP-2) and osteoblast functions in three-dimensional titanium alloy scaffolds: stimulation of osteogenic activity, J. Biomed. Mater. Res. A (2015), http://dx.doi.org/10.1002/jbm.a.35592.

[17] H. Hosseinkhani, M. Hosseinkhani, A. Khademhosseini, H. Kobayashi, Bone regeneration through controlled release of bone morphogenetic protein-2 from 3-D tissue engineered nano-scaffold, J. Control. Release 117 (2007) 380–386.
[18] Z.Y. Lin, Z.X. Duan, X.D. Guo, J.F. Li, H.W. Lu, Q.X. Zheng, D.P. Quan, S.H. Yang, Bone induction by biomimetic PLGA-(PEG-ASP) n copolymer loaded with a novel synthetic BMP-2-related peptide in vitro and in vivo, J. Control. Release 144 (2010) 190–195.
[19] J.R. Lieberman, A. Daluiski, T.A. Einhorn, The role of growth factors in the repair of bone. Biology and clinical applications, J. Bone Joint Surg. Am. 84-A (2002) 1032–1044.
[20] O. Jeon, S.J. Song, H.S. Yang, S.H. Bhang, S.W. Kang, M.A. Sung, J.H. Lee, B.S. Kim, Long-term delivery enhances in vivo osteogenic efficacy of bone morphogenetic protein-2 compared to short-term delivery, Biochem. Biophys. Res. Commun. 369 (2008) 774–780.
[21] X.F. Niu, P. Chen, G. Zhou, Z.D. She, R.W. Tan, M.B. Wang, Y.B. Fan, Ectopic osteogenesis of a microsphere-scaffold delivery system with encapsulated synthetic peptide derived from BMP-2, J. Control. Release 172 (2013) E135.
[22] Q. Li, G. Zhou, X. Yu, T. Wang, Y. Xi, Z. Tang, Porous deproteinized bovine bone scaffold with three-dimensional localized drug delivery system using chitosan microspheres, Biomed. Eng. Online 14 (2015) 33, http://dx.doi.org/10.1186/s12938-015-0028-2.
[23] G.B. Wei, Q.M. Jin, W.V. Giannobile, P.X. Ma, Nano-fibrous scaffold for controlled delivery of recombinant human PDGF-BB, J. Control. Release 112 (2006) 103–110.
[24] Z. Li, L. Kupcsik, S.J. Yao, M. Alini, M.J. Stoddart, Chondrogenesis of human bone marrow mesenchymal stem cells in fibrin-polyurethane composites, Tissue Eng. Part A 15 (2009) 1729–1737.
[25] J.A. Sanz-Herrera, M. Doblare, J.M. Garcia-Aznar, Scaffold microarchitecture determines internal bone directional growth structure: a numerical study, J. Biomech. 43 (2010) 2480–2486.
[26] T.B. Woodfield, J. Malda, J. de Wijn, F. Peters, J. Riesle, C.A. van Blitterswijk, Design of porous scaffolds for cartilage tissue engineering using a three-dimensional fiber-deposition technique, Biomaterials 25 (2004) 4149–4161.
[27] L. Ciocca, F. De Crescenzio, M. Fantini, R. Scotti, CAD/CAM and rapid prototyped scaffold construction for bone regenerative medicine and surgical transfer of virtual planning: a pilot study, Comput. Med. Imaging Graph. 33 (2009) 58–62.
[28] J.A. Peres, T. Lamano, Strategies for stimulation of new bone formation: a critical review, Braz. Dent. J. 22 (2011) 443–448.
[29] O. Jeon, S.J. Song, S.W. Kang, A.J. Putnam, B.S. Kim, Enhancement of ectopic bone formation by bone morphogenetic protein-2 released from a heparin-conjugated poly(L-lactic-*co*-glycolic acid) scaffold, Biomaterials 28 (2007) 2763–2771.
[30] X. Xu, A.K. Jha, R.L. Duncan, X. Jia, Heparin-decorated, hyaluronic acid–based hydrogel particles for the controlled release of bone morphogenetic protein 2, Acta Biomater. 7 (2011) 3050–3059.
[31] I. Pountos, T. Georgouli, K. Henshaw, H. Bird, E. Jones, P.V. Giannoudis, The effect of bone morphogenetic protein-2, bone morphogenetic protein-7, parathyroid hormone, and platelet-derived growth factor on the proliferation and osteogenic differentiation of mesenchymal stem cells derived from osteoporotic bone, J. Orthop. Trauma 24 (2010) 552–556.
[32] Z.S. Haidar, R.C. Hamdy, M. Tabrizian, Delivery of recombinant bone morphogenetic proteins for bone regeneration and repair. Part A: current challenges in BMP delivery, Biotechnol. Lett. 31 (2009) 1817–1824.
[33] B. Li, T. Yoshii, A.E. Hafeman, J.S. Nyman, J.C. Wenke, S.A. Guelcher, The effects of rhBMP-2 released from biodegradable polyurethane/microsphere composite scaffolds on new bone formation in rat femora, Biomaterials 30 (2009) 6768–6779.
[34] K.V. Brown, B. Li, T. Guda, D.S. Perrien, S.A. Guelcher, J.C. Wenke, Improving bone formation in a rat femur segmental defect by controlling bone morphogenetic protein-2 release, Tissue Eng. Part A 17 (2011) 1735–1746.
[35] R.E. Geuze, L.F. Theyse, D.H. Kempen, H.A. Hazewinkel, H.Y. Kraak, F.C. Oner, W.J. Dhert, J. Alblas, A differential effect of bone morphogenetic protein-2 and vascular endothelial growth factor release timing on osteogenesis at ectopic and orthotopic sites in a large-animal model, Tissue Eng. Part A 18 (2012) 2052–2062.
[36] Q. Zhang, K. Tan, Y. Zhang, Z. Ye, W.S. Tan, M. Lang, In situ controlled release of rhBMP-2 in gelatin-coated 3D porous poly(epsilon-caprolactone) scaffolds for homogeneous bone tissue formation, Biomacromolecules 15 (2014) 84–94.
[37] T.J. Cho, L.C. Gerstenfeld, T.A. Einhorn, Differential temporal expression of members of the transforming growth factor beta superfamily during murine fracture healing, J. Bone Miner. Res. 17 (2002) 513–520.
[38] G. Ragetly, D.J. Griffon, Y.S. Chung, The effect of type II collagen coating of chitosan fibrous scaffolds on mesenchymal stem cell adhesion and chondrogenesis, Acta Biomater. 6 (2010) 3988–3997.
[39] X.B. Yang, R.S. Bhatnagar, S. Li, R.O. Oreffo, Biomimetic collagen scaffolds for human bone cell growth and differentiation, Tissue Eng. 10 (2004) 1148–1159.
[40] F.J. Xu, Y.Q. Zheng, W.J. Zhen, W.T. Yang, Thermoresponsive poly(N-isopropyl acrylamide)-grafted polycaprolactone films with surface immobilization of collagen, Colloids Surf. B: Biointerfaces 85 (2011) 40–47.
[41] T.A. Mahmood, R. de Jong, J. Riesle, R. Langer, C.A. van Blitterswijk, Adhesion-mediated signal transduction in human articular chondrocytes: the influence of biomaterial chemistry and tenascin-C, Exp. Cell Res. 301 (2004) 179–188.
[42] B.C. Cooley, R.A. Daley, J.M. Toth, Long-term BMP-2-induced bone formation in rat island and free flaps, Microsurgery 25 (2005) 167–173.